Detection of anomalous diffusion using confidence intervals of the scaling exponent with application to preterm neonatal heart rate variability

David R. Bickel,* M. Terese Verklan, and Jon Moon
Health Science Center at Houston, The University of Texas, Suite 4.430, 1100 Holcombe Boulevard, Houston, Texas 77030
(Received 4 May 1998)

The scaling exponent of the root mean square (rms) displacement quantifies the roughness of fractal or multifractal time series; it is equivalent to other second-order measures of scaling, such as the power-law exponents of the spectral density and autocorrelation function. For self-similar time series, the rms scaling exponent equals the Hurst parameter, which is related to the fractal dimension. A scaling exponent of 0.5 implies that the process is normal diffusion, which is equivalent to an uncorrelated random walk; otherwise, the process can be modeled as anomalous diffusion. Higher exponents indicate that the increments of the signal have positive correlations, while exponents below 0.5 imply that they have negative correlations. Scaling exponent estimates of successive segments of the increments of a signal are used to test the null hypothesis that the signal is normal diffusion, with the alternate hypothesis that the diffusion is anomalous. Dispersional analysis, a simple technique which does not require long signals, is used to estimate the scaling exponent from the slope of the linear regression of the logarithm of the standard deviation of binned data points on the logarithm of the number of points per bin. Computing the standard error of the scaling exponent using successive segments of the signal is superior to previous methods of obtaining the standard error, such as that based on the sum of squared errors used in the regression; the regression error is more of a measure of the deviation from power-law scaling than of the uncertainty of the scaling exponent estimate. Applying this test to preterm neonate heart rate data, it is found that time intervals between heart beats can be modeled as anomalous diffusion with negatively correlated increments. This corresponds to power spectra between $1/f^2$ and $1/f$, whereas healthy adults are usually reported to have $1/f$ spectra, suggesting that the immaturity of the neonatal nervous system affects the scaling properties of the heart rate. [S1063-651X(98)14911-5]

PACS number(s): 87.10.+e, 05.40.+j

I. INTRODUCTION

Power-law scaling has been used to describe signals of physical systems as diverse as turbulence [1,2], the stock market [3,4], geophysical phenomena [5], heart rate variability [6–10], DNA sequence composition [11–13], and, more recently, DNA evolution [although they are related, DNA sequence composition must be distinguished from DNA evolution since the former deals with spatial autocorrelations (see Ref. [14]), whereas the latter deals with temporal autocorrelations. A critical point process with scaling in time may result from the self-organization of interacting genes [15]] [16–19]. A defining characteristic of fractal or multifractal time series is the growth of the second-order structure function, also called the variogram [5], as a power law in the time between increments:

$$\langle [x(t_i)-x(t_j)]^2 \rangle \propto |t_i-t_j|^{2H}, \tag{1}$$

where i and j are integers that index times, and H is a positive real parameter. The increments are assumed to have a mean of zero:

$$\langle x(t_i)-x(t_j) \rangle = 0. \tag{2}$$

For self-affine (monofractal) time series, H is the Hurst exponent, named after Edwin Hurst for his study of river heights [20]. The Hurst exponent completely characterizes the scaling properties of self-affine time series, and is related to the fractal dimension by $D=E-H+1$, where E is the Euclidean dimension of the signal [21]. Although the second-order exponent H is only one of the infinite number of structure function exponents of a multifractal process [5], H is important as a descriptive parameter in that it measures the scaling in second-order functions such as the spectral density and autocorrelation. A generalization of the Wiener-Khintchine theorem for nonstationary processes [5] yields the power spectral density

$$S(f) \sim \frac{1}{f^{2H+1}} \tag{3}$$

for the range of frequencies f corresponding to the time scales for which Eq. (1) holds. Increments can be treated as the first derivative of a smoothed signal, leading to a spectral density of increments proportional to $(f^{2H-1})^{-1}$, which, again using the Wiener-Khintchine theorem [22], provides the autocorrelation $\Phi(\tau)$ in the increments of a signal,

$$\Phi(\tau) \sim \frac{1}{|\tau|^{2(1-H)}}, \tag{4}$$

valid for lag times τ corresponding to the frequencies of Eq. (3). The last step assumes the stationarity of the increment process, requiring that $0 \leqslant H < 1$; Mandelbrot and van Ness noted this restriction on the Hurst exponent of fractal Brownian motion, a self-affine process with stationary increments

*Electronic address: BickelDR@aol.com

called fractal Brownian noise [23]. The autocorrelation (4) is positive for $H>0.5$, negative for $H<0.5$, and zero for $H=0.5$, the case of normal diffusion (Brownian motion) or an uncorrelated random walk. A process with $H\neq 0.5$ can be modeled as anomalous diffusion or as a correlated continuous time random walk; see Refs. [24–26] for relationships between the two formalisms. Alternately, discrete-event counts that scale as Eq. (3) can be described as fractal-rate stochastic point processes [27].

Several techniques for estimating H have been proposed, including rescaled-range (R/S) analysis [20], autocorrelation analysis [28,29], dispersional analysis [30], spectral analysis [31], wavelet analysis [32,5], wavelet packet analysis [33], detrended fluctuation analysis [7,10], maximum likelihood analysis [34], and, for point processes, Allan-Fano factor analysis [Fano factor analysis [35,9,36], a method related to Allan-Fano factor analysis, does not directly estimate H since it applies to stationary event counts with power spectra between $1/f^1$ and $1/f^0$, rather than to nonstationary event counts with power spectra given by Eq. (3)] [37,38,9,27]. Using synthetically generated fractal Brownian motion signals, dispersional and spectral analyses usually yield lower bias and higher precision (statistical efficiency) in the estimates of H than rescaled-range and correlation analyses [39]. When comparing the dispersional method to the spectral method, the former yields better results when the fractal signal is generated using a covariance matrix [40], while the latter performs better when the signal is generated using spectral synthesis [39] (Appendix A). Maximum likelihood estimation has lower bias and higher precision than other methods [39,40], but the time complexity of the optimization involved makes it less practical [39]. Although the proposed test is compatible with all of these estimation techniques, we use dispersional analysis herein because it is simple and because the effects of short signal lengths and additive white noise on the dispersional estimation of H have been studied numerically [21].

II. DISPERSIONAL ANALYSIS

Dispersional analysis provides an estimate of the scaling exponent from the dependence of the standard deviation of binned data on the bin sizes. In this method, a time series S_{L+1} consisting of $L+1$ measurements, $\hat{x}(t_i)$, sampled at times $t_i=i\Delta t(i=1,2,\ldots,L+1)$, is differenced to obtain a vector of increments S' defined by

$$S'\equiv(\xi_1,\xi_2,\ldots,\xi_L), \tag{5}$$

where each increment is the difference between two successive measurements:

$$\xi_i\equiv\hat{x}(t_{i+1})-\hat{x}(t_i) \quad \text{with } i=1,2,\ldots,L. \tag{6}$$

S' is partitioned into N disjoint sets of m increments per set; N is the greatest integer less than or equal to L/m. The elements of each bin are averaged to yield a time series S'_m of N values y_{mj}:

$$S'_m\equiv(y_{m,1},y_{m,2},\ldots,y_{m,N}), \tag{7}$$

where

$$y_{m,j}\equiv\frac{1}{m}\sum_{i=(j-1)m+1}^{jm}\xi_i=\frac{\hat{x}(t_{jm+1})-\hat{x}(t_{(j-1)m+1})}{m} \quad \text{for } j=1,2,\ldots,N. \tag{8}$$

Assuming that the signal follows Eq. (2), the increment expected mean is zero ($\langle\xi\rangle=0$), and thus the sample standard deviation of S' at resolution m can be defined as

$$\hat{\sigma}_m\equiv\left(\frac{1}{N}\sum_{j=1}^{N}y_{m,j}^2\right)^{1/2}. \tag{9}$$

This differs from the sample standard deviation definition which is typically used in dispersional analysis [41], and which would be more appropriate if the expected mean were unknown:

$$\hat{\sigma}_m(\text{unknown}\langle\xi\rangle)\equiv\left[\frac{1}{N-1}\sum_{j=1}^{N}\left(y_{m,j}-\frac{1}{N}\sum_{j=1}^{N}y_{m,j}\right)^2\right]^{1/2}. \tag{10}$$

Combining Eqs. (8) and (9) yields

$$\hat{\sigma}_m=\frac{1}{m}\left\{\frac{1}{N}\sum_{j=1}^{N}[\hat{x}(t_{jm+1})-\hat{x}(t_{(j-1)m+1})]^2\right\}^{1/2}. \tag{11}$$

The sample standard deviation $\hat{\sigma}_m$ is an unbiased estimator of the expected standard deviation at resolution m, which, using Eq. (1), is

$$\sigma_m\equiv\frac{1}{m}\{\langle[x(t_{jm+1})-x(t_{(j-1)m+1})]^2\rangle\}^{1/2}=\frac{C}{m}(|t_m-t_0|^{2H})^{1/2}=\frac{C}{m}(m\Delta t)^H=\frac{\sigma_1}{m^{1-H}}, \tag{12}$$

where C is a constant of proportionality. Taking the logarithm of Eq. (12) yields a straight line with slope $-(1-H)$ and intercept $\log\sigma_1$:

$$\log\sigma_m=-(1-H)\log m+\log\sigma_1. \tag{13}$$

Dispersional analysis uses sample standard deviations $\hat{\sigma}_m$ to obtain estimates of H and σ_1, respectively $\hat{H}$ and $\hat{\sigma}$, through linear regression by minimizing the sum of squared errors:

$$\varepsilon^2\equiv\sum_{m=m_{\min},2m_{\min},4m_{\min},\ldots,m_{\max}/2,m_{\max}}[-(1-\hat{H})\log m+\log\hat{\sigma}-\log\hat{\sigma}_m]^2 \quad \text{for } 1\leqslant m_{\min}<m_{\max}\leqslant\frac{L}{16}. \tag{14}$$

The range of bin sizes m is determined by selecting minimum and maximum bin sizes, $m_{\min}$ and $m_{\max}$, for which Eq. (12) holds; $m_{\max}$ has an upper limit of $L/16$, since sample standard deviations $\hat{\sigma}_m$ are unreliable estimates of population standard deviations σ_m for larger m [41]. Bin sizes for which $\hat{\sigma}_m = 0$ must be excluded from the analysis [41] because the logarithm of zero is undefined.

III. CONFIDENCE INTERVALS AND HYPOTHESIS TESTING

In using the estimated value $\hat{H}$ as a descriptive statistic, confidence intervals can be obtained using its estimated standard error $\hat{\sigma}_{\hat{H}}$. The standard error can also be used to test the hypothesis that a time series is normal diffusion as opposed to anomalous diffusion. After discussing two widely used methods of computing $\hat{\sigma}_{\hat{H}}$, we introduce a third technique that combines the advantages of the previous methods.

Standard errors are typically calculated in one of two ways. The first method equates the estimated standard error of $\hat{H}$ with that of the estimated slope $-(1-\hat{H})$ obtained from the minimized squared error ε^2 of the regression

$$\hat{\sigma}_{\hat{H}}(\varepsilon) \equiv \left(\frac{n\varepsilon^2}{(n-2)^2[n\Sigma_m(\log m)^2 - (\Sigma_m \log m)^2]} \right)^{1/2}, \tag{15}$$

where n is the number of bin sizes m that are used in regression (14) and in the sums of Eq. (15). This method apparently has the advantage that the standard error can be estimated from a single time series. However, $\hat{\sigma}_{\hat{H}}(\varepsilon)$ is more of a measure of the deviation of the data from Eq. (12) than it is an accurate measure of the variability in $\hat{H}$. This unreliability is evident from previous uses of the technique. For example, Bassingthwaighte and Raymond [21] used Eq. (15) to compute $\hat{\sigma}_{\hat{H}}(\varepsilon)$ for three synthetically generated data sets, of length 2^{13} points each, with $H = 0.2$, 0.5, and 0.8. In the second case, they obtained $\hat{H} = 0.54$ and $\hat{\sigma}_{\hat{H}} = 0.012$, which implies that the true H value of 0.5 lies well outside the 95% confidence interval of $\hat{H}$, and that the null hypothesis that $H = 0.5$ would thus be wrongly rejected, assuming that the errors of the regression are independent and normally distributed. The residuals, however, actually strongly violate independence, as is seen by the typical systematic oscillations of $\log \hat{\sigma}_m$ around the line of regression, which partly explains why $\hat{\sigma}_{\hat{H}}(\varepsilon)$ performs so poorly as a measure of the variation in $\hat{H}$.

Bassingthwaighte and Raymond [21] noted that the standard deviation of many $\hat{H}$ values provides a stronger estimate of the variability in $\hat{H}$ than does Eq. (15) using a single value of $\hat{H}$. If $\hat{H}_i$ is the estimate of the scaling exponent for the ith of M time series assumed to have the same scaling exponent H, then the estimate of H is the sample mean of the $\hat{H}_i$ values,

$$\hat{H} \equiv \frac{1}{M} \sum_{i=1}^{M} \hat{H}_i, \tag{16}$$

and the estimated standard error in that estimate is the sample standard deviation divided by the square root of the sample size:

$$\hat{\sigma}_{\hat{H}} \equiv \left(\frac{1}{M(M-1)} \sum_{i=1}^{M} (\hat{H}_i - \hat{H})^2 \right)^{1/2}. \tag{17}$$

The standard error $\hat{\sigma}_{\hat{H}}$ can be used to compute confidence intervals and test hypotheses using the t distribution if the population of $\hat{H}_i$ values is normal, an assumption that holds for independent dispersional estimates of the scaling exponent of fractal Brownian motion [21]. Even without assuming normality, $\hat{\sigma}_{\hat{H}}$ is a useful measure of uncertainty in that, by Chebychev's inequality, the probability that the scaling exponent falls outside the range $\hat{H} \pm K\hat{\sigma}_{\hat{H}}$ is less than or equal to $1/K^2$ for any distribution. The drawback of this technique is that it requires multiple time series that are known *a priori* to have the same fractal scaling.

We propose the partition method, a one-series variant of the multiple-estimate method of computing $\hat{\sigma}_{\hat{H}}$. The ML increments of a single fractal time series S_{ML+1} are partitioned into M nonoverlapping subseries of L increments each. Then, for $i = 1,2,\ldots,M$, dispersional analysis is used to obtain $\hat{H}_i$, the estimate the scaling exponent of the ith increment subseries. The estimate of H for the original time series, $\hat{H}$, is found using Eq. (16) and the standard error $\hat{\sigma}_{\hat{H}}$ is found using Eq. (17). This method combines the strengths of the two techniques described above in that it provides a good estimate of the variability in the estimate of the scaling exponent while requiring only one time series.

The standard error in the scaling exponent estimate can be used to test hypotheses about the scaling exponent H of a fractal time series S_{ML+1}. The most important question in this regard is whether a data set can be modeled as normal diffusion ($H = 0.5$) or anomalous diffusion ($H \neq 0.5$), since the increments of the former are uncorrelated, whereas those of the latter have positive ($H > 0.5$) or negative ($H < 0.5$) autocorrelations [Eq. (4)]. One could test the null hypothesis that $H = 0.5$ using the z test with $\hat{H}$ and $\hat{\sigma}_{\hat{H}}$, but this is unreliable since for finite data lengths L because $\hat{H}$ is a biased estimator of H [21], i.e., $\hat{H}$ from Eq. (16) does not asymptotically approach H as $M \to \infty$. Thus, instead of comparing $\hat{H}$ to 0.5, it is more meaningful to compare $\hat{H}$ to $\hat{H}^{\text{Brown}}$, the dispersional analysis estimate of H for simulated ordinary Brownian motion ($H = 0.5$). Since the increments of Brownian motion (normal diffusion) are independent and normally distributed, the estimates of the scaling exponent, $\hat{H}^{\text{Brown}}$, and that of its standard error, $\hat{\sigma}_{\hat{H}}^{\text{Brown}}$, can be computed from the dispersional analysis of M^{Brown} series of L computer-generated Gaussian random numbers of zero mean and unit standard deviation. Then $\hat{H}^{\text{Brown}}$ and $\hat{\sigma}_{\hat{H}}^{\text{Brown}}$ are, respectively, the sample mean and standard error in the mean of the M^{Brown} estimates, $\hat{H}_i^{\text{Brown}}$, with each estimate obtained by the dispersional analysis of a stochastic series of length L. The estimates $\hat{H}$ and $\hat{H}^{\text{Brown}}$ must be computed using the same value of L since the bias in estimates of H depends strongly on the number of increments used [21]. We use $\langle \hat{H} \rangle$ and $\langle \hat{H}^{\text{Brown}} \rangle$ to denote expectation values of estimates, that is

$$\langle \hat{H} \rangle \equiv \lim_{M \to \infty} \frac{1}{M} \sum_{i=1}^{M} \hat{H}_i \tag{18}$$

and

$$\langle \hat{H}^{\mathrm{Brown}} \rangle \equiv \lim_{M^{\mathrm{Brown}} \to \infty} \frac{1}{M^{\mathrm{Brown}}} \sum_{i=1}^{M^{\mathrm{Brown}}} \hat{H}_i^{\mathrm{Brown}}. \tag{19}$$

The original time series S_{ML+1} is ordinary Brownian motion if $\langle \hat{H} \rangle = \langle \hat{H}^{\mathrm{Brown}} \rangle$, positively correlated anomalous diffusion if $\langle \hat{H} \rangle > \langle \hat{H}^{\mathrm{Brown}} \rangle$, or negatively correlated anomalous diffusion if $\langle \hat{H} \rangle < \langle \hat{H}^{\mathrm{Brown}} \rangle$. Thus the null hypothesis h_0 is that $\langle \hat{H} \rangle = \langle \hat{H}^{\mathrm{Brown}} \rangle$ with the alternate hypothesis $h_a : \langle \hat{H} \rangle \neq \langle \hat{H}^{\mathrm{Brown}} \rangle$. This test of the equality of population means is performed using the two-tailed, pooled (two-sample) t test [22] using the sample means $\hat{H}$ and $\hat{H}^{\mathrm{Brown}}$ and the standard errors $\hat{\sigma}$ and $\hat{\sigma}^{\mathrm{Brown}}$. This test is used to determine whether, for a series S_{ML+1}, the increment autocorrelation (4) measured by $\hat{H}$ is statistically significant, and, if so, whether it is positive or negative. Section IV illustrates the use of the test with heart rate data. Alternately, one could compute $\hat{H}$ directly from the original data without partitioning, and use that estimate with $\hat{H}^{\mathrm{Brown}}$ and $\hat{\sigma}^{\mathrm{Brown}}$ in a two-tailed, one-sample t test to test h_0 and h_a, but then the uncertainty ($\hat{\sigma}$) in $\hat{H}$ would be unavailable.

In theory, one could similarly test other hypotheses about the scaling exponent of a time series S_{ML+1}, for example, whether $H=0$, in which case Eq. (3) implies that the power spectrum goes like $1/f^1$; this is sometimes called flicker noise. Then dispersional analysis would be applied to series of $1/f^1$ fluctuations to obtain the scaling exponent's sample mean $\hat{H}^{\mathrm{flicker}}$ and standard error of the mean $\hat{\sigma}^{\mathrm{flicker}}$. These values would be used in place of $\hat{H}^{\mathrm{Brown}}$ and $\hat{\sigma}^{\mathrm{Brown}}$ in the above procedure in order to determine whether $\hat{H}$ is significantly different from $\hat{H}^{\mathrm{flicker}}$, which would mean that S_{ML+1} does not have a $1/f^1$ spectrum. However, this test has limited reliability because the bias in the estimate $\hat{H}^{\mathrm{flicker}}$ has a strong dependence on the method used to simulate the $1/f^1$ fluctuations, since, in general, biases in estimating the scaling exponent vary widely when using different techniques of fractal Brownian motion generation [40]. The test works best when the null hypothesis is ordinary Brownian motion because simulations of normal diffusion ($H=0.5$) are superior to those of anomalous diffusion ($H \neq 0.5$).

An alternate test of whether an estimate from a fractal time series indicates a significant deviation in H from 0.5 is based on estimates of the scaling exponent after reshuffling the increments. Using an estimation technique equivalent to dispersional analysis, Mantegna [4] found that $\hat{H}$, the estimate of H for a stock index time series, is 0.57 ± 0.02, while $\hat{H}^{\mathrm{shuffled}}$, the estimate for the same data randomly blended in time, is only 0.49 ± 0.01. He concluded that $\hat{H}$ differed significantly from $\hat{H}^{\mathrm{shuffled}}$, and that there was therefore coupling between the price and time. However, his confidence intervals were presumably computed with Eq. (15), which, as argued above, is a highly unreliable measure of uncertainty. This test could be improved by randomly reordering the increments a large number of times, and then computing $\hat{H}^{\mathrm{shuffled}}$ as the sample mean and $\hat{\sigma}^{\mathrm{shuffled}}$ as the standard error of the mean of the scaling exponent estimates of the reshuffled data increments. Then the one-sided, one-sample t test could be applied using $\hat{H}$, $\hat{H}^{\mathrm{shuffled}}$, and $\hat{\sigma}^{\mathrm{shuffled}}$ to determine whether the time series being tested is normally diffusive ($H=0.5$), superdiffusive ($H>0.5$), or subdiffusive ($H<0.5$). The two-sample t test could be used instead if the time series is partitioned, so that $\hat{H}$ and $\hat{\sigma}$ are the sample mean and standard error of the estimates from the subseries. Testing H using the reshuffling technique directly determines whether there is significant autocorrelation [Eq. (4)] in the data increments without requiring a comparison to simulated Brownian motion. Nonetheless, the method of comparing $\hat{H}$ to $\hat{H}^{\mathrm{Brown}}$ is preferred when multiple time series are tested because $\hat{H}^{\mathrm{Brown}}$ only has to be computed once, whereas, in the reordering method, $\hat{H}^{\mathrm{shuffled}}$ must be recomputed for each time series. Using the same standard of comparison $\hat{H}^{\mathrm{Brown}}$ for all data sets is computationally efficient and enables consistent hypothesis testing from data set to data set.

IV. APPLICATION TO HEART RATE VARIABILITY

The estimation of the scaling exponent of the adult human heart rate has received considerable attention over the last two decades. The most popular estimation method is spectral analysis, which indirectly estimates H since anomalous diffusion has the spectrum $S(f)$ given by Eq. (3). For healthy subjects, many researchers (e.g., Refs. [7,10,9]) report spectra close to $S(f) \sim 1/f^1$, equivalent to $H \approx 0$, while others [8] report $S(f) \sim 1/f^2$, equivalent to $H \approx 0.5$ (normal diffusion). Subjects with congestive heart failure tend to have elevated scaling exponents [7,8,9]; for example, Peng *et al.* [7] found that they are closer to $H \approx 0.5$. Obtaining reliable confidence intervals of H and statistically testing the hypothesis that $H=0.5$ can potentially resolve discrepancies in the literature while facilitating the prediction of patients' health.

We used dispersional analysis with hypothesis testing to statistically quantify scaling in the neonatal heart rate. Since the parasympathetic nervous system of neonates is not yet completely developed, their nervous control of the heart beat differs dramatically from that of adults. Comparing the scaling exponent of adults to that of neonates would reveal the extent to which this difference affects the scaling properties of the heart rate.

The times between heartbeats (R-R intervals) of 13 preterm neonates were measured for approximately 10 min weekly for ten weeks, beginning when the neonates had a postconceptional age of 26 weeks and ending when they were 35 weeks old. Thus, there would be 130 series of interbeat intervals, but 11 of the series could not be recorded, due either to a medical condition or a discharge before week 35, so a total of 119 series were analyzed. Appendix B describes the data collection. Each series of successive interevent times is treated as a time series for the purposes of dispersional analysis, even though the independent variable is the interval number rather than the time of measurement. The interval number is not converted to units of time, as this would cause information to be lost in the interpolation of the intervals.

$\hat{H}$, the estimate of the scaling exponent H, and $\hat{\sigma}_{\hat{H}}$, the

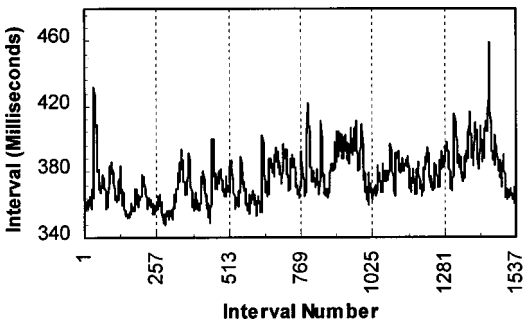

FIG. 1. Tachogram: Interbeat interval vs interval number for a very healthy neonate (VH1 of Table I), measured at a postconceptional age of 35 weeks. As mentioned in the text, intervals beyond 1537 were discarded and are not shown. The subject was not on ventilator or oxygen support at the time of measurement, and thus was breathing autonomously. Increments were obtained for dispersional analysis by subtracting each interval from its subsequent interval. Figure 2 illustrates the dispersional analysis of the first and third subseries of 256 increments.

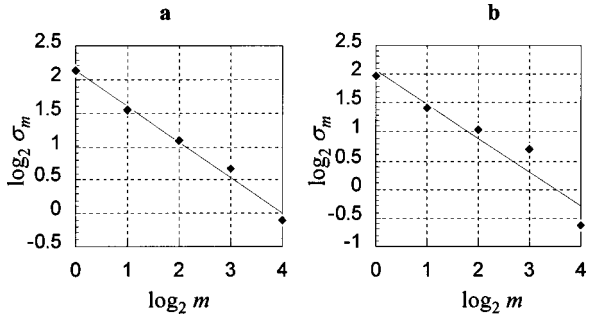

FIG. 2. Dispersional analysis plots: Logarithm of standard deviation vs logarithm of bin size, with regression lines. Dispersional analysis is performed on each 256-increment segment of the data plotted in Fig. 1 to estimate the scaling exponent of that data. Plots for two such segments are displayed here. (a) Dispersional analysis plot using the first 256 increments of the data displayed in Fig. 1. The close fit of the regression line to the data is quantified by the standard error of the slope, which, based on Eq. (15), is only 0.031. This standard error satisfies condition (21), so the slope of -0.531 is added to 1 to obtain 0.469 as the estimate of the scaling exponent for the segment of 256 increments. This estimate was averaged with estimates from the other three increment segments that satisfied condition (21) to obtain the estimate and standard error of the scaling exponent for the series of Fig. 1. These values are in the upper-right corner of Table I, and are plotted as the last point and error bounds of Fig. 3. (b) Dispersional analysis plot using increments 513–768 of the data displayed in Fig. 1. The poor fit of the regression line to the data is quantified by the standard error of the slope, which, based on Eq. (15), is 0.102. This high standard error does not satisfy condition (21), so the slope was not used to estimate the scaling exponent.

standard error of the estimate, were computed for each interval series using the partition method described in Sec. III. First, the increments ε_i for each series were obtained using

$$\varepsilon_i \equiv \hat{x}_{i+1} - \hat{x}_i , \tag{20}$$

where $\hat{x}_i$ is the ith time interval between two successive heartbeats. Then each increment series was partitioned into M subseries of 256 increments each ($L=256$), discarding the increments at the end of each increment series, i.e., only the increments ε_i for which $i \leqslant ML$ were analyzed. Dispersional analysis was performed on each increment subseries with Eqs. (7)–(14), to obtain scaling exponent estimates $\hat{H}_i$ for $i=1,2,\ldots,M$, using bin sizes m from $m_{\min}=1$ to $m_{\max}=16$. Since dispersional analysis assumes that the standard deviations of binned data scale as Eq. (12), each estimate $\hat{H}_i$ was regarded as reliable if its regression error ε_i was small enough to satisfy

$$\hat{\sigma}_{\hat{H}_i}(\varepsilon_i) < 1/10, \tag{21}$$

where $\hat{\sigma}_{\hat{H}_i}(\varepsilon_i)$ is defined by Eq. (15) with $n=5$. Of the 703 increment subseries available, 635 yielded reliable estimates of the scaling exponent. Redefining M as the number of reliable estimates for an increment series, $\hat{H}$ and $\hat{\sigma}_{\hat{H}}$ were obtained for each of 119 original interval series using Eqs. (16) and (17) with the reliable estimates $\hat{H}_i$. One of the interval series is displayed in Fig. 1, and the estimation of the scaling exponent of that series is illustrated in Fig. 2. Figure 3 shows the estimated exponents and exponent standard errors for all series of one neonate, including the series of Fig. 1. The corresponding results for all neonates are displayed in Table I. Consistent with Refs. [7–9], the mean scaling exponent of ''very healthy'' subjects is less than that of other subjects, but this is not statistically significant. The scaling exponent estimates are not significantly correlated with age.

In determining whether an interval series is Brownian motion (an uncorrelated random walk), $\hat{H}$ and $\hat{\sigma}_{\hat{H}}$ were used with their counterparts from simulated Brownian increments in a two-sample, one-sided t test, as outlined in Sec. III. We found the sample mean ($\hat{H}^{\text{Brown}}=0.488$) and standard error of the mean ($\hat{\sigma}_{\hat{H}}^{\text{Brown}}=0.001$) of 5000 values $\hat{H}_i^{\text{Brown}}$, the estimate of the scaling exponent for the ith series of 256 independent Gaussian random numbers with zero mean and unit standard deviation. [Of the 5000 estimates, only two of them violated Eq. (21), so their effect on $\hat{H}^{\text{Brown}}$ and $\hat{\sigma}^{\text{Brown}}$ are negligible.] Using the values of Table I, a comparison of $\hat{H}^{\text{Brown}}$ to $\hat{H}$ for each series indicates that at the 0.1% (respectively 1%) significance level, the null hypothesis $h_0:\langle\hat{H}\rangle=\langle\hat{H}^{\text{Brown}}\rangle$ was rejected for seven (respectively 21) of 119 series, and $\hat{H}<\hat{H}^{\text{Brown}}$ in all significant cases. At the 5% level, h_0 was rejected for 42 series, 41 of which satisfied $\hat{H}<\hat{H}^{\text{Brown}}$. Therefore, the null hypothesis could be rejected 5.9% of the time at the 0.1% level, 17.6% of the time at the 1% level, and 35.3% of the time at the 5% level. The facts that each percentage of null rejections is several times the corresponding significance level and that $\hat{H}<\hat{H}^{\text{Brown}}$ in all or nearly all significant cases require that many of the interval series be modeled as subdiffusion ($H<0.5$) rather than normal diffusion.

For purposes of comparison, this test was also applied to 1000 series, each consisting of 1536 independent Gaussian random numbers of zero mean and unit standard deviation, using $L=256$ and $M=6$, the median number of subseries per increment series for the heart interval data analyzed. The null hypothesis h_0 of this synthetic data set could be rejected one time (only 0.1% of the time) at the 0.1% level, with $\hat{H}$

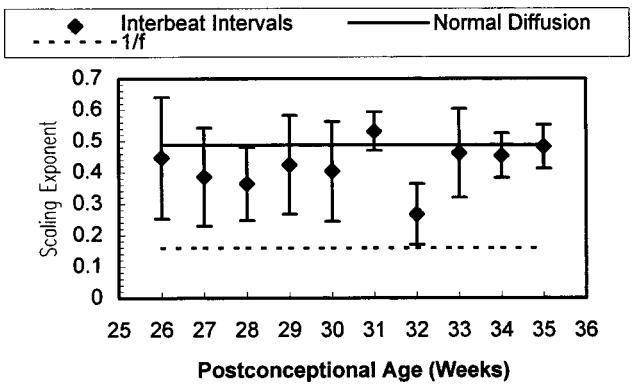

FIG. 3. Scaling exponent estimates: Scaling exponent estimates of the interbeat intervals of a very healthy neonate (VH1 of Table I). Error bars were computed using twice the standard error of the mean scaling exponent in order to roughly estimate 95% confidence intervals. Figure 2 illustrates how the mean and standard error of the scaling exponent were estimated at the 35th week; other weeks were treated similarly. The horizontal lines give the mean simulated scaling exponent values for 256-increment segments of normal diffusion (uncorrelated random walk) and a random signal with a $1/f^1$ power spectrum; the standard errors of these exponents are smaller than the widths of the lines. All estimates of the scaling exponent are below the estimate for normal diffusion, except for the estimate at a postconceptional age of 31. However, only the estimate of the scaling exponent at 32 weeks deviates significantly from that of normal diffusion. The points plotted are the numbers in the first row of Table I.

$>\hat{H}^{\mathrm{Brown}}$; h_0 could be rejected 13 times (only 1.3% of the time) at the 1% level, with two significant occurrences of $\hat{H}<\hat{H}^{\mathrm{Brown}}$; and h_0 could be rejected 61 times (only 6.1% of the time) at the 5% level, with 23 significant occurrences of $\hat{H}<\hat{H}^{\mathrm{Brown}}$. These results are as expected: the percentages of null rejections are approximately equal to the significance levels, and the numbers of rejections on each side of the t distribution are comparable. Thus there are substantial differences between the synthetic Brownian motion and the heartbeat interval data, both in the percentage of h_0 rejections and in the proportion of rejections corresponding to $\langle\hat{H}\rangle < \langle\hat{H}^{\mathrm{Brown}}\rangle$.

Since the power spectrum of the healthy adult heart intervals are usually considered to be approximately $1/f^1$, we addressed the question of whether this holds for neonates by comparing estimates of the scaling exponent for flicker noise, $\hat{H}^{\mathrm{flicker}}$, to $\hat{H}$ for each series studied. Using the spectral synthesis method of generating data with a $1/f^1$ spectrum (Appendix A), $\hat{H}^{\mathrm{flicker}}=0.159$ and $\hat{\sigma}^{\mathrm{flicker}}=0.001$ are the sample mean and standard error of the mean of 5000 estimates of the scaling exponent of $1/f^1$ fluctuations of 256 points each. (Excluding the 115 estimates that violated condition (21) would lead to $\hat{H}^{\mathrm{flicker}}=0.162$ and $\hat{\sigma}^{\mathrm{flicker}}=0.001$.) The large bias in the estimate $\hat{H}^{\mathrm{flicker}}$ is evident from Eq. (3), which implies that $H\approx 0$ for a $1/f^1$ spectrum. As can be seen from Table I, $\hat{H}$ typically ranges from $\hat{H}^{\mathrm{flicker}}$ to $\hat{H}^{\mathrm{Brown}}$; hence, according to Eq. (3), the spectrum of the neonatal interbeat intervals varies between $1/f^2$ and $1/f^1$. Flicker noise was not statistically tested as a null hypothesis, since the value of $\hat{H}^{\mathrm{flicker}}$ depends heavily on the method of $1/f^1$ spectrum generation.

V. DISCUSSION AND CONCLUSIONS

Using the partition method of estimating the standard error of the scaling exponent, we found that a statistically significant number of preterm neonatal heartbeat series are subdiffusive ($H<0.5$). Neonatal beat-to-beat dynamics range between $1/f^1$ fluctuations ($H=0$) and normal diffusion ($H=0.5$) on a scale of $m_{\mathrm{min}}=1$ beat to $m_{\mathrm{max}}=16$ beats. Iyengar *et al.* [10] found that the healthy young adult heartbeat has an approximately $1/f^1$ power spectrum on a scale between four and 30 beats, which would imply that the scaling exponent is generally higher for preterm neonates than for adults. The preterm neonate intervals thus appear to be closer to an uncorrelated random walk, whereas the adult interval increments have stronger negative autocorrelations [Eq. (4)]. We hypothesize that *the difference in the heart rate scaling between neonates and adults reflects the immaturity of the neonatal autonomic nervous system*. In particular, the parasympathetic nervous system (vagus) is not fully developed until a year after birth. It is likely that, during the maturation of the nervous system, the increasing regulation of the heart by the vagus causes the heartbeat increments to become more negatively correlated, as is quantified by a lower scaling exponent. (A negative correlation in the interval increments means that an increase in the time between successive beats is likely to be followed by a decrease, and vice versa.) This idea is compatible with that of Iyengar *et al.* [10], who suggested that the decreased negative autocorrelation of old adults as compared to young adults may be due partly to reduced vagal control of the heart in old adults. It is interesting that the $1/f^1$ heartbeat dynamics of healthy young adults seem to be largely absent from humans with either underdeveloped or deteriorating autonomic nervous systems. Further research is needed here, since there is disagreement over the presence of $1/f^1$ fluctuations in adults [8], and since different analysis methods were used in studying neonates and adults. Using the above method and time scale in the study of adults would shed light on the differences between neonatal and adult heartbeat dynamics. Our hypothesis could also be tested by comparing structure function exponents other than the second-order exponent of Eq. (1) since the heart rate in general is not strictly self-affine, but has evidence of multifractal scaling [42].

The application to short heart rate signals illustrates the simplicity and utility of the partition method in estimating the standard error of scaling exponents and in testing the hypothesis of normal diffusion. This technique can similarly lead to a better understanding of the correlation properties of other time series known to be scaling in the structure function [Eq. (1)], power spectrum [Eq. (3)], or autocorrelation function [Eq. (4)].

ACKNOWLEDGMENTS

We would like to thank Joseph P. Zbilut of Rush College of Medicine for helpful discussions. This research was supported in part (for MTV) by the Bristol Myers Squibb Foundation and the American Nurses Foundation.

APPENDIX A: FAST GENERATION OF FRACTAL SIGNALS

Fractal signals can be generated using spectral synthesis [43], the method often employed in studies of dispersional

TABLE I. Hurst exponent estimates of preterm neonatal interbeat intervals. Hurst exponent estimates and standard errors displayed are the sample mean and standard error of the mean of M estimates, each obtained from the dispersional analysis of a segment of 256 successive increments of time intervals between heart beats. The regression error of each estimate is small enough that condition (21) is satisfied. ''VHi'' denotes the ith neonate classed as very healthy (healthy without oxygen support), ''MHi'' denotes the ith neonate classed as moderately healthy (healthy with oxygen support), ''MUi'' denotes the ith neonate classed as moderately unhealthy (unhealthy but not always on a ventilator), and ''VUi'' denotes the ith neonate classed as very unhealthy (unhealthy and on a ventilator for entire study); health classifications are described in Appendix B. Weeks 26–35 are the postconceptional ages of the neonate at the times of measurement. ''Mean for health status'' gives the mean and standard error of the mean of the Hurst exponent estimates listed for a given health status, and ''Mean for age'' gives the mean and standard error of the mean of the Hurst exponent estimates listed for a given postconceptional age. The lower right cell gives the mean and standard error of the mean of all Hurst exponent estimates listed. Significance levels were obtained by comparison to $\hat{H}^{\text{Brown}}=0.488\pm0.001$, as described in the text. N/A: Data are not available. *Significantly larger than $\hat{H}^{\text{Brown}}$ at the 5% level.

$\hat{H}\pm\hat{\sigma}_{\hat{H}}$	Week 26	Week 27	Week 28	Week 29	Week 30	Week 31	Week 32	Week 33	Week 34	Week 35	Mean for health status	Mean for health status
VH1	0.447 ±0.097 ($M=4$)	0.387 ±0.078 ($M=5$)	0.364 ±0.058 ($M=5$)	0.425 ±0.079 ($M=5$)	0.404 ±0.080 ($M=4$)	0.532 ±0.031 ($M=6$)	0.267[a] ±0.048 ($M=4$)	0.462 ±0.071 ($M=6$)	0.454 ±0.036 ($M=6$)	0.483 ±0.035 ($M=4$)		
VH2	0.421 ±0.034 ($M=4$)	0.496 ±0.049 ($M=3$)	0.251[b] ±0.031 ($M=5$)	0.543 ±0.087 ($M=4$)	0.421[a] ±0.025 ($M=6$)	0.297[a] ±0.060 ($M=7$)	0.329[b] ±0.039 ($M=6$)	0.465 ±0.044 ($M=6$)	0.449 ±0.046 ($M=5$)	0.522 ±0.036 ($M=6$)		
VH3	N/A	0.403[a] ±0.024 ($M=6$)	0.490 ±0.072 ($M=8$)	0.403[a] ±0.024 ($M=6$)	0.445 ±0.039 ($M=6$)	0.488 ±0.027 ($M=6$)	0.393[a] ±0.024 ($M=5$)	0.570 ±0.040 ($M=3$)	0.418[a] ±0.019 ($M=6$)	0.272[b] ±0.040 ($M=6$)		
VH4	0.330[c] ±0.018 ($M=6$)	0.377 ±0.038 ($M=4$)	0.367 ±0.08 ($M=6$)	0.409 ±0.047 ($M=5$)	0.507 ±0.031 ($M=5$)	0.524 ±0.020 ($M=5$)	0.551 ±0.038 ($M=6$)	0.496 ±0.027 ($M=5$)	N/A	N/A	0.388[c] ±0.014 (very healthy)	0.388[c] ±0.014 (very healthy)
VH5	N/A	0.410 ±0.103 ($M=6$)	0.248[b] ±0.048 ($M=6$)	0.500 ±0.074 ($M=5$)	0.438 ±0.128 ($M=6$)	0.241[c] ±0.038 ($M=7$)	0.306 ±0.103 ($M=5$)	0.511 ±0.069 ($M=5$)	0.359 ±0.053 ($M=6$)	0.256[a] ±0.071 ($M=6$)		
VH6	−0.075[c] ±0.040 ($M=5$)	0.379[a] ±0.031 ($M=5$)	0.140 ±0.034 ($M=2$)	0.325 ±0.069 ($M=6$)	0.419 ±0.046 ($M=4$)	0.186[c] ±0.040 ($M=6$)	0.326[a] ±0.037 ($M=5$)	0.350[b] ±0.030 ($M=6$)	0.458 ±0.026 ($M=4$)	N/A		
VH7	N/A	0.264[c] ±0.011 ($M=4$)	0.262[b] ±0.051 ($M=6$)	0.338[b] ±0.035 ($M=6$)	0.288[b] ±0.047 ($M=6$)	0.372 ±0.059 ($M=5$)	0.500 ±0.046 ($M=6$)	0.392 ±0.067 ($M=6$)	0.357[a] ±0.037 ($M=5$)	0.433 ±0.043 ($M=5$)		
MH1	0.267[a] ±0.069 ($M=6$)	0.541 ±0.033 ($M=4$)	0.508 ±0.043 ($M=5$)	0.548 ±0.028 ($M=6$)	0.480 ±0.024 ($M=6$)	0.583 ±0.045 ($M=6$)	0.502 ±0.051 ($M=8$)	0.228[a] ±0.067 ($M=5$)	0.548 ±0.033 ($M=6$)	0.430 ±0.043 ($M=6$)		
MH2	0.199[b] ±0.039 ($M=5$)	0.290[a] ±0.049 ($M=6$)	0.391 ±0.052 ($M=5$)	0.430 ±0.023 ($M=5$)	0.443 ±0.050 ($M=5$)	0.388 ±0.060 ($M=6$)	0.353[a] ±0.042 ($M=6$)	0.532 ±0.074 ($M=7$)	N/A	0.343 ±0.080 ($M=5$)	0.421[a] ±0.027 (moder. healthy)	
MU1	0.401 ±0.043 ($M=8$)	0.409 ($M=1$)	0.258[b] ±0.027 ($M=4$)	0.472 ±0.053 ($M=4$)	0.330[a] ±0.045 ($M=5$)	0.168[c] ±0.035 ($M=5$)	0.487 ±0.168 ($M=3$)	0.464 ±0.034 ($M=6$)	0.180[c] ±0.027 ($M=6$)	N/A		0.417[c] ±0.015 (all except very healthy)
MU2	N/A	0.292[b] ±0.028 ($M=5$)	0.435[a] ±0.019 ($M=6$)	0.499 ±0.068 ($M=6$)	0.384 ±0.067 ($M=4$)	0.587* ±0.037 ($M=6$)	0.515 ±0.038 ($M=4$)	0.523 ±0.037 ($M=7$)	0.567 ±0.038 ($M=5$)	0.564 ±0.034 ($M=7$)	0.491[a] ±0.030 (moder. unhlthy.)	

TABLE I. (*Continued*).

$\hat{H}\pm\hat{\sigma}_{\hat{H}}$	Week 26	Week 27	Week 28	Week 29	Week 30	Week 31	Week 32	Week 33	Week 34	Week 35	Mean for health status	Mean for health status
VU1	0.502 $\pm$0.023 ($M=6$)	0.338[b] $\pm$0.020 ($M=5$)	0.502 $\pm$0.023 ($M=6$)	0.454 $\pm$0.039 ($M=6$)	0.439 $\pm$0.050 ($M=4$)	N/A	0.516 $\pm$0.029 ($M=6$)	0.467 $\pm$0.028 ($M=5$)	0.398 $\pm$0.069 ($M=4$)	0.359 $\pm$0.056 ($M=6$)		
VU2	N/A	0.485 $\pm$0.056 ($M=6$)	0.278[a] $\pm$0.048 ($M=5$)	0.514 $\pm$0.068 ($M=4$)	0.503 $\pm$0.039 ($M=6$)	0.398[a] $\pm$0.030 ($M=7$)	0.219[b] $\pm$0.060 ($M=6$)	0.459 $\pm$0.037 ($M=5$)	0.371[b] $\pm$0.010 ($M=4$)	0.211[a] $\pm$0.063 ($M=5$)	0.412[b] $\pm$0.023 (very unhlthy.)	
Mean for Age	0.312[a] $\pm$0.065	0.390[a] $\pm$0.023	0.346[c] $\pm$0.032	0.451[a] $\pm$0.020	0.423[b] $\pm$0.017	0.397[a] $\pm$0.043	0.405[b] $\pm$0.031	0.455 $\pm$0.025	0.414[a] $\pm$0.032	0.387[a] $\pm$0.038		0.402[c] $\pm$.010 (overall)

[a]Significantly smaller than A^{Brown} at the 5% level.
[b]Significantly smaller than A^{Brown} at the 1% level.
[c]Significantly smaller than A^{Brown} at the 0.1% level.

analysis [21,39]. We modify the method of Saupe [43] to enable efficient computations using the fast Fourier transform (FFT); Voss also used FFT in simulating fractal Brownian motion [44]. The idea is to obtain a fractal time series $(\hat{x}_1,\hat{x}_2,\ldots,\hat{x}_l)$ of even length l from random Fourier coefficients $(\tilde{x}_{-l/2},\tilde{x}_{-(l/2)+1},\ldots,\tilde{x}_{l/2})$ with a spectral density that scales according to the chosen exponent β, i.e.,

$$S_k \propto |\tilde{x}_k|^2 \sim \frac{1}{k^{\beta}}, \tag{A1}$$

with each positive integer k corresponding to the frequency k/l. The amplitudes and phases of the coefficients are randomized, so that

$$\tilde{x}_k = \begin{cases} \left(\dfrac{G_k}{k^{-\beta/2}}\right)\exp(i\phi_k), & 1 \leqslant k \leqslant l/2 \\ 0, & -l/2 \leqslant k \leqslant 0, \end{cases} \tag{A2}$$

where G_k is a Gaussian random number of zero mean and fixed standard deviation, and ϕ_k is a random number uniformly distributed between 0 and 2π. The fractal time series is the real part of the discrete inverse Fourier transform of the random coefficients:

$$\hat{x}_j = \mathrm{Re}\left[\frac{1}{l}\sum_{k=-l/2}^{l/2}\tilde{x}_k \exp\left(-i\,\frac{2\pi jk}{l}\right)\right] \quad \text{for } j=1,2,\ldots,l. \tag{A3}$$

If l is chosen to be an integer power of 2, then Eq. (A3) can be computed quickly using the FFT algorithm [22]. Since fractal Brownian motion has a power spectrum given by Eq. (3), spectral synthesis can be used to generate a fractal signal of a given scaling exponent H by setting $\beta=2H+1$. Similarly, a $1/f^1$ signal can be generated by letting $\beta=1$.

An artifact of the spectral synthesis method is that the first and last points ($\hat{x}_1$ and $\hat{x}_l$) are strongly correlated. This effect can be minimized by generating a fractal series that is much longer than the one needed, and then retaining only a portion of it. For example, of the 5000 $1/f^1$ signals generated for the computation of $\hat{H}^{\text{flicker}}$, as described in Sec. IV, 2500 were the first 257 values of signals of length $l=2048$, generated with the FFT. The other 2500 signals were generated without truncation, using the first 257 values of signals of length $l=258$ (the speed of the FFT is not needed for such small series). Applying Eq. (6) to each signal yielded increment series of length $L=257-1=256$. Bassingthwaighte and Raymond [21] used a similar method of combining the scaling exponent estimates from signals with and without truncation.

APPENDIX B: DATA COLLECTION AND NEONATE HEALTH STATUSES

The data used herein was studied previously in an investigation of the pattern of neurodevelopment in the preterm infants. The heart rate data was recorded from a three lead electrocardiograph (ECG) digitized at 250 Hz via a MiniLogger™ (Sunriver, OR) connected to a Nonin 8800 cardiorespiratory monitor. Data was collected between 7 and 9 a.m. for each neonate. The researcher verified that each neonate had not been disturbed for the 30 min prior to the data collection. The Anderson Behavioral State Scale, a measure the neonate's behavioral state, was recorded by hand at 1-min intervals. A total of 119 10-min physiological recordings of the ECG were obtained from the 13 neonates over the ten-week period. Artifacts were detected and edited manually.

Thirty-five weeks of postconceptional age was chosen as the measuring point for delineating health status because preterm neonates are typically discharged home at this time if eating well and displaying a steady weight gain. The health status categories were defined by the usual parameters utilized in clinical practice. The very healthy neonates were tolerating full feeds, exhibiting steady weight gain, required no ventilatory support, were not receiving supplemental oxygen, were on no medications, and were awaiting discharge.

The moderately healthy neonates, although receiving full feeds and exhibiting steady weight gain, still required supplemental oxygen, and were not ready for discharge. The moderately unhealthy neonates were receiving a combination of hyperalimentation and enteral nutrition, medication (Tobramycin, Vancomycin, and Theophylline) and supplemental oxygen. The very unhealthy neonates still required the use of mechanical ventilation and oxygen to maintain homeostasis, and also required medication (Amikacin, Albuterol, Aminophylline, Ceftazidime, Cisapride, Lasix, Fentanyl, Tobramycin, and Amphotericin *B*) and hyperalimentation.

The medical conditions of the neonates included respiratory distress and sepsis early in life, and as each infant grew, the medical conditions either resolved or became chronic (bronchopulmonary dysphasia and continued ventilatory support). Every infant was treated with theophylline during the course of hospital stay. All infants with a gestational age greater than 26 weeks, inappropriate growth for gestational age, received vasopressors, presence of congenital anomalies, intraventricular hemorrhage greater than grade II, or substance abuse exposed by maternal history were excluded from the study.

[1] M. F. Shlesinger, B. J. West, and J. Klafter, Phys. Rev. Lett. **58**, 1100 (1987).

[2] J. F. Muzy, E. Bacry, and A. Arneodo, Phys. Rev. Lett. **67**, 3515 (1991).

[3] B. B. Mandelbrot, J. Polit. Econ. **71**, 421 (1963).

[4] R. N. Mantegna, Physica A **179**, 232 (1991).

[5] A. Davis, A. Marshak, and W. Wiscombe, in *Wavelets in Geophysics*, edited by E. Foufoula-Georgiou and P. Kumar (Academic, San Diego, 1994).

[6] A. L. Goldberger, D. R. Rigney, and B. J. West, Sci. Am. **262**, 42 (1990).

[7] C. K. Peng, S. Havlin, H. E. Stanley, and A. L. Goldberger, Chaos **5**, 82 (1995).

[8] J. P. Zbilut, M. Zak, and C. L. Webber, Chaos Solitons Fractals **5**, 1509 (1995).

[9] R. G. Turcott and M. C. Teich, Ann. Biomed. Eng. **24**, 269 (1996).

[10] N. Iyengar, C. K. Peng, R. Morin, A. L. Goldberger, and L. A. Lipsitz, Am. J. Physiol. **271**, R1078 (1996).

[11] S. V. Buldyrev, N. V. Dokholyan, A. L. Goldberger, S. Havlin, C.-K. Peng, H. E. Stanley, and G. M. Viswanathan, Physica A **249**, 430 (1998).

[12] A. Arnéodo, Y. D'Aubenton-Carafa, B. Audit, E. Bacry, J. F. Muzy, and C. Thermes, Physica A **249**, 439 (1998).

[13] P. Allegrini, M. Buiatti, P. Grigolini, and B. J. West, Phys. Rev. E **57**, 4558 (1998).

[14] J. W. Fickett, D. C. Torney, and D. R. Wolf, Genomics **13**, 1056 (1992).

[15] D. R. Bickel (unpublished).

[16] D. R. Bickel and B. J. West, Mol. Biol. Evol. **15**, 967 (1998).

[17] D. R. Bickel and B. J. West, Fractals **6**, 211 (1998).

[18] D. R. Bickel and B. J. West, J. Mol. Evol. (to be published November 1998).

[19] B. J. West and D. R. Bickel, Physica A **249**, 544 (1998).

[20] H. E. Hurst, Trans. Am. Soc. Civ. Eng. **116**, 770 (1951).

[21] J. B. Bassingthwaighte and G. M. Raymond, Ann. Biomed. Eng. **23**, 491 (1995).

[22] W. H. Press, S. A. Teukolsky, W. T. Vetterling, and B. P. Flannery, *Numerical Recipes* (Cambridge University Press, Cambridge, 1995).

[23] B. B. Mandelbrot and J. W. van Ness, SIAM (Soc. Ind. Appl. Math.) Rev. **10**, 422 (1968).

[24] A. Compte, Phys. Rev. E **53**, 4191 (1996).

[25] B. J. West, P. Grigolini, R. Metzler, and T. F. Nonnenmacher, Phys. Rev. E **55**, 99 (1997).

[26] R. Metzler and T. F. Nonnenmacher, Phys. Rev. E **57**, 6409 (1998).

[27] S. Thurner, S. B. Lowen, M. C. Feurstein, C. Heneghan, H. G. Feigchtinger, and M. C. Teich, Fractals **5**, 565 (1997).

[28] P. A. Burrough, J. Soil Sci. **34**, 577 (1983).

[29] P. A. Burrough, J. Soil Sci. **34**, 599 (1983).

[30] J. B. Bassingthwaighte, News Physiol. Sci. **3**, 5 (1988).

[31] M. S. Keshner, Proc. IEEE **70**, 212 (1982).

[32] L. M. Kapplan and C. C. Jay Kuo, IEEE Trans. Signal Process **41**, 3554 (1993).

[33] C. L. Jones, G. T. Longergan, and D. E. Mainwaring, J. Phys. A **29**, 2509 (1996).

[34] T. Lundahl, W. J. Ohley, S. M. Kay, and R. Siffert, IEEE Trans. Med. Imaging **MI-5**, 152 (1986).

[35] D. H. Johnson and A. R. Kumar, J. Mol. Evol. **47**, 1353 (1990).

[36] S. B. Lowen and M. C. Teich, Fractals **3**, 183 (1995).

[37] M. C. Teich, C. Heneghan, S. B. Lowen, and R. G. Turcott, in *Wavelets in Medicine and Biology*, edited by A. Aldroubi and M. Unser (CRC Press, New York, 1996), pp. 383–412.

[38] P. Abry and P. Flandrin, in *Wavelets in Medicine and Biology* (Ref. [37]), pp. 413–437.

[39] H. E. Schepers, J. H. G. M. van Beek, J. B. Bassingthwaighte, IEEE Eng. Med. Biol. Mag. **11**, 57 (1992).

[40] R. Fischer and M. Akay, Ann. Biomed. Eng. **24**, 537 (1996).

[41] G. Raymond, Dispersional analysis code and comments available at http://nsr.bioeng.washington.edu/NSR/NSRinfo/avsoftware/NSR_SW_fractal.html (1994).

[42] D. R. Bickel (unpublished).

[43] D. Saupe, in *The Science of Fractal Images*, edited by H. O. Peitgen and D. Saupe (Springer-Verlag, New York, 1988).

[44] R. F. Voss, in *The Science of Fractal Images* (Ref. [43]).